Supporting Information

Enabling Isotope Ratio Measurements on an Ion Trap Mass Spectrometer

Timothy Vazquez, Colette Taylor, Maverick Knowlton, Sean Williams and Theresa Evans-Nguyen*

Department of Chemistry, University of South Florida, 4202 East Fowler Avenue, Tampa, Florida 33620, United States

Corresponding Author Email: evansnguyen@usf.edu

Table of Contents

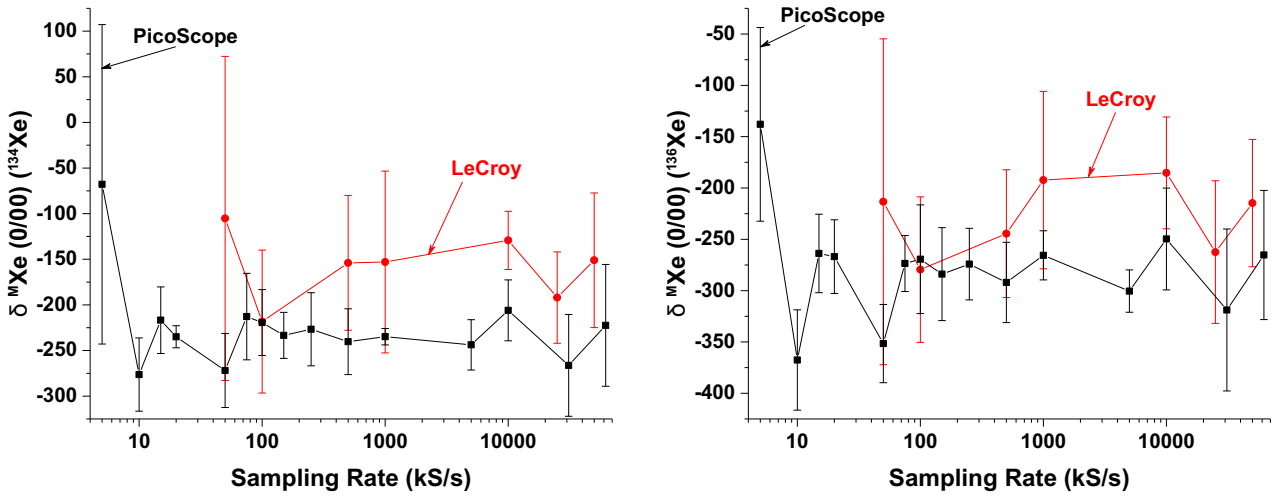

Figure S1: Per mille deviations of a) ^{134}Xe and b) ^{136}Xe at varied sampling rates on the PicoScope DAQ (black) and LeCroy DAQ (red).

A study of the x-axis resolution on both the LeCroy and PicoScope DAQs was performed to determine optimal operating conditions. It was found that on either DAQ, no trend of precision or accuracy improvement was observed. The sampling rate study reported in Figure S-1 did not in fact yield any obvious trends to explain the optimal x-axis sampling conditions (in contrast to our results for y-axis resolution enhancement). We presume that faster sampling rates do not provide improvements in area calculations because faster timing resolution is not entirely analogous to the enhanced voltage resolution. For the peak area calculation, the FWHM of each peak is generally the same (~< 1 ms) and does not span a wide dynamic range, unlike voltage intensity which we observe to span 3 orders-of-magnitude. Additionally, the absolute error in time may simply correspond to the jitter of the scope (~ps) such that the relative error contribution is only ~ 10^{-9} and is likely insignificant compared to more prominent sources of error.

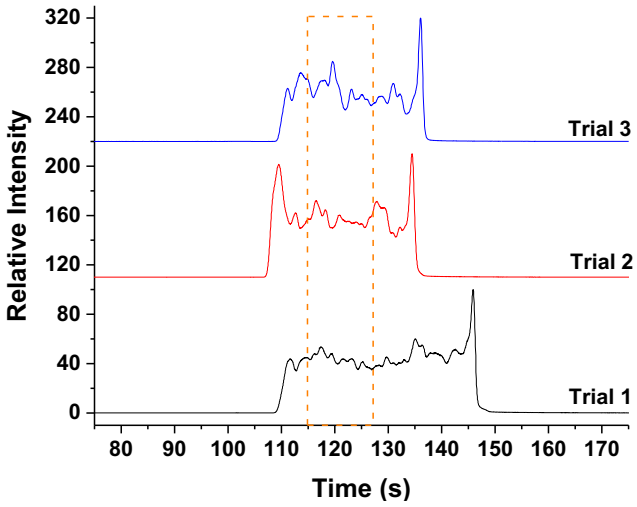

Figure S2: GC-QTOF chromatograms for triplicate manual injections of xenon from lecture bottle showing averaged 250 scans (dashed red box).

Calibration of the lecture bottle of xenon was necessary to infer isotope ratios from the measurements taken by the DIT. Manual injections of xenon were introduced in triplicate with a precision headspace syringe (Valco) to a TOF instrument (Agilent 7200 GC-QTOF) provided by the University's Core Mass Spectrometry Facility. Representative samplings of xenon were then extracted from the chromatographs ensuring no detector saturation.

	Atmospheric Isotope Ratio, R_{ref} (Basford, 1973)		TOF Integrated Signal			Isotope Ratio (R_M) from TOF Trials Referenced to ^{130}Xe peak			per mille dev relative to atmospheric xenon (δ^MXe)	
ISOTOPE	^{m}Xe / ^{132}Xe	^{m}Xe / ^{130}Xe	**Trial 1**	**Trial 2**	**Trial 3**	**R_M Avg**	**R_M StDev**	**RSD**	**‰ Avg**	**‰ StDev**
124	0.35	2.337	19.87	29.24	30.08	1.608	0.025	1.551	-311.69	10.68
126	0.33	2.180	20.31	29.63	30.08	1.628	0.041	2.527	-253.39	18.87
128	7.14	47.15	492.38	733.24	754.22	40.173	0.349	0.868	-147.90	7.40
129	98.32	649.6	7412.81	10930.32	11194.67	600.003	9.433	1.572	-76.32	14.52
130	**15.14**	100.0	1213.52	1835.67	1885.52	100.000	0.000	0.000	0.00	0.00
131	*78.90*	*521.3*	*6206.78*	*9115.45*	*9338.21*	*501.100*	*9.002*	*1.796*	*-38.70*	*17.27*
132	100.00	660.7	8271.39	12168.89	12451.94	668.304	11.584	1.733	11.54	17.53
134	38.79	256.3	3281.96	4845.06	4970.88	266.008	3.849	1.447	37.97	15.02
136	32.94	217.6	2822.56	4196.13	4296.42	229.682	2.547	1.109	55.39	11.70

Table S1: Summary of TOF integrated signal and per mille deviation from theoretical values of atmospheric xenon according to Basford et al., 1973.

Data from the literature were transformed from isotope ratios relative to ^{132}Xe to isotope ratios relative to ^{130}Xe, to serve as the atmospheric reference R_{Ref}, following the format of Pepin. From the pseudo-chromatographic data, averaged xenon spectra were extracted. The averaged spectra were then translated into the measured isotope ratios R_M. To determine isotopic abundances, the area under the curve for each isotopic peak was calculated and compared to the area of the reference isotope (^{130}Xe). An example calculation for the per mille deviation is provided below from data corresponding to isotope ^{131}Xe, Trial 1:

$$\text{Trial 1 Isotope Ratio}\frac{131\text{Xe}}{130\text{Xe}}: \qquad \mathrm{R}_M = \left(\frac{6206.78}{1213.52}\right) \times 100 = 511.50$$

$$\delta^M\text{Xe} = 1000 \times \left(\left(\frac{R_M}{R_{Ref}}\right) - 1\right) = 1000 \times \left(\left(\frac{511.50}{521.3}\right) - 1\right) = -18.80\ ‰$$

Upon visual comparison, the lecture bottle of xenon was found to have significant variations from reference Earth atmospheric abundances. Figure S3 depicts the values in Table S1. It is believed that the purification process of commercial sources of xenon results in isotope fractionation which accounts for deviations from true atmospheric samples. (CIAAW. **Isotopic compositions of the elements 2019**. Available online at www.ciaaw.org.) Figure S3 appears to reflect a general artifact of xenon production-the relative depletion of the lighter isotopes and enrichment of heavier isotopes. Therefore, we note that the comparison of per mille deviations to Earth Atmospheric xenon should not be taken to inform on the accuracy of the TOF measurements.

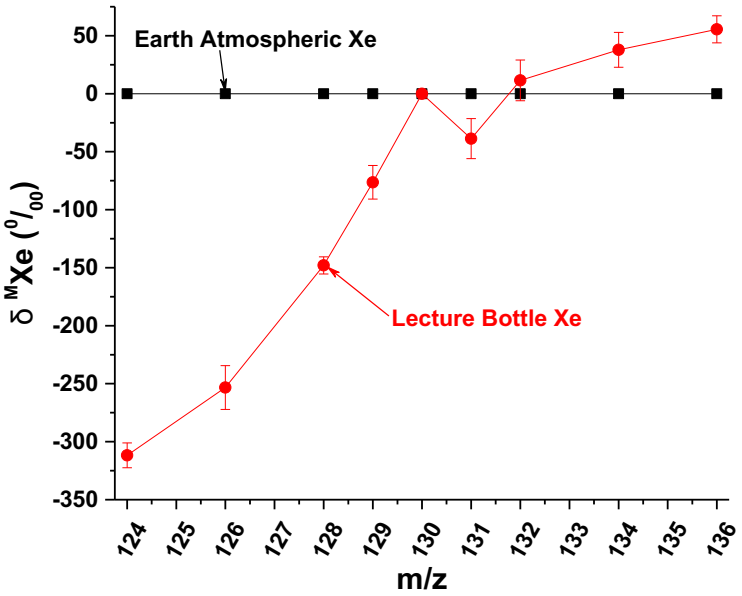

Figure S3: Composition of earth atmospheric Xe (black) and lecture bottle Xe,(red) normalized to ^{130}Xe and shown as per mille ($^{0}/_{00}$) deviations from atmospheric Xe compositions.

m/z	^{124}Xe	^{126}Xe	^{128}Xe	^{129}Xe	^{130}Xe	^{131}Xe	^{132}Xe	^{134}Xe	^{136}Xe
DIT LeCroy	ND	ND	41.23 ± 6.55	765.66 ± 106.35	100	694.98 ± 87.24	919.04 ± 124.90	275.10 ± 33.74	233.99 ± 24.19
DIT PicoScope	ND	ND	39.63 ± 4.29	754.93 ± 49.77	100	671.35 ± 41.80	903.20 ± 62.85	274.98 ± 12.83	235.79 ± 17.93
TOF-Xe	1.61 ± 0.02	1.63 ± 0.04	40.17 ± 0.35	600.00 ± 9.43	100	501.10 ± 9.00	668.30 ± 1.58	266.00 ± 3.85	229.68 ± 2.55

Table S2: Isotope ratios of DIT xenon and lecture bottle xenon derived from QTOF standardization. All isotopes are referenced to ^{130}Xe ≡ 100 and undetected ions are represented by ND.

We suspected detector nonlinearity was a possible explanation for the variance from the atmospheric values shown in Figure S3. Without a quantitative reference standard to calibrate the Agilent detector we cursorily attributed the observed deviations to potential saturation in the TOF's microchannel plate. To test this theory internally, we plot below in Figure S4 the expected TOF abundance ratio versus the expected theoretical atmospheric xenon abundance ratios because the xenon isotope abundances naturally span almost 3 orders of magnitude. As shown below, an orange trendline featuring an R^2 of 0.999 is comprised of just the lowest 6 abundances, and extrapolated to the highest three abundances, the isotopes of ^{131}Xe, ^{129}Xe, and ^{132}Xe. Meanwhile, a blue trendline featuring a poorer R^2 of 0.9958 is comprised of all 9 abundances. Arguably, we observe the potential beginning of a nonlinear response of TOF signal relative to the orange trendline. Assuming the orange trendline is accurate, the extrapolation to high abundances would reveal a bias for ^{129}Xe, ^{131}Xe, and ^{132}Xe yielding underestimation of these isotopes. Such a bias would explain the trend observed in Figure 3b when applied to the trap. That is, relative to the TOF-calibrated lecture bottle, the DIT ratios would appear to overestimate those isotopes. Nonetheless, without a deliberate calibration of the TOF detector, we cannot fully verify this hypothesis.

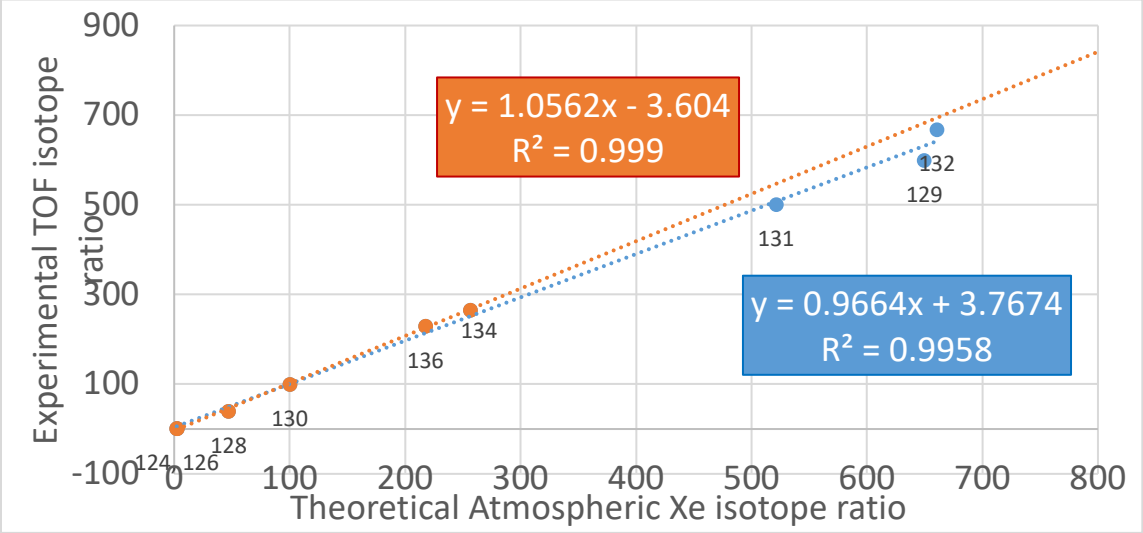

Figure S4: Correlation between the linearity of TOF isotope ratios and theoretical isotope ratios of xenon using all isotopes (blue) and lower abundance isotopes only (orange).

A y-axis resolution study was performed to determine the effects of bit resolution on the precision of measurements provided by the DAQ. From this study, a trend of improved precision was observed as the y-axis resolution was increased. Accuracy also shows an improvement with a limit reached above 12 bits y-axis resolution.

Static Buffer Gas Introduction		**δ ^{M}Xe**	
DAQ System	**Bit Resolution (bits)**	**^{134}Xe ($^{0}/_{00}$)**	**^{136}Xe ($^{0}/_{00}$)**
LeCroy	8	34.2 ± 126.8	18.8 ± 105.3
PicoScope	8	33.7 ± 48.2	26.6 ± 78.0
	12	17.7 ± 69.7	16.7 ± 34.0
	14	11.0 ± 29.2	2.0 ± 29.3
	15	-0.7 ± 16.3	7.7 ± 8.2
	16	2.6 ± 2.1	0.5 ± 1.0

Table S3: Y-axis resolution study, per mille deviations for both the LeCroy and PicoScope DAQs at varied bit resolutions.

To validate system performance, we crudely modified our system to decrease the LMCO and enable the observation of our chemical noise simulant, argon. While isotopic resolution was lost, qualitative observations of argon and xenon individually and in a mixture indicated that we were able to trap both compounds.

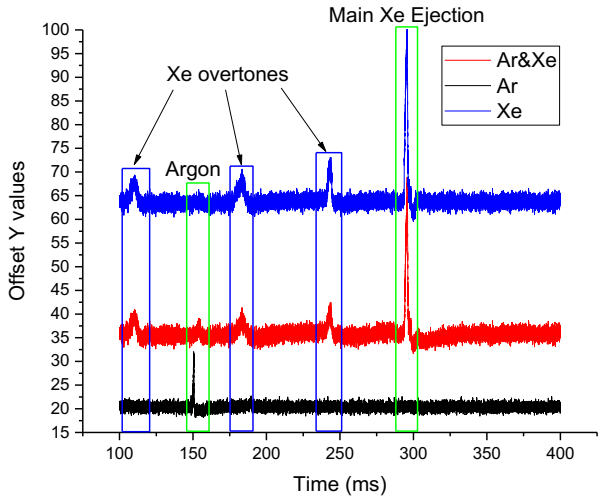

Figure S5: Mass spectra of argon (black), xenon (blue) and an argon/xenon mixture (red) at a trapping voltage of 440 V_{RF}.

Under our optimized conditions where isotopic resolution is obtained we then compared our sample using a simulated atmospheric sample. With argon present as a source of chemical noise and introduction of a 1:1 argon : xenon mixture we compared our precision and accuracy to that pure xenon. From this study it was found that the overall signal intensity dropped slightly in the mixture, but the precision and accuracy were maintained.

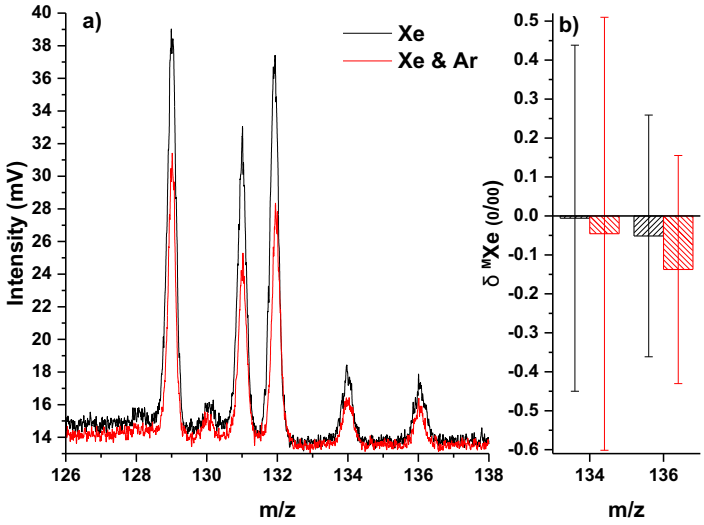

Figure S6: a) Mass spectra and b) per mille deviations at ^{134}Xe and ^{136}Xe of xenon (black) and an argon/xenon mixture (red) at a trapping voltage of 600 V_{RF}.

During the re-coupling of our pulsed buffer gas introduction with the higher bit resolution detection we encountered detector sensitivity problems for an additional y-axis resolution study. Nonetheless, we found that for our targeted isotopes of ^{134}Xe and ^{136}Xe, the same trend in improvements was observed as seen in static buffer gas introduction. The detector sensitivity unfortunately compromised calculations for all other peak intensities and thereby potential improvements in precision and accuracy across the broader dynamic range.

Pulsed Buffer Gas Introduction		**δ ^{M}Xe (‰)**					
DAQ System	**Bit Resolution**	**^{128}Xe**	**^{129}Xe**	**^{131}Xe**	**^{132}Xe**	**^{134}Xe**	**^{136}Xe**
LeCroy	8	-241.7 ± 115.5	1175.2 ± 213.3	1111.2 ± 204.4	882.2 ± 185.6	45.1 ± 108.7	38.6 ± 110.7
PicoScope	8	-276.8 ± 355.6	995.3 ± 147.7	920.0 ± 152.9	660.7 ± 136.0	75.4 ± 70.6	35.4 ± 38.0
	12	-956.6 ± 39.8	894.9 ± 74.9	799.2 ± 63.7	537.3 ± 61.3	20.9 ± 35.7	17.1 ± 41.4
	14	-332.4 ± 120.3	967.8 ± 35.4	921.3 ± 53.6	628.7 ± 41.8	0.9 ± 17.6	9.5 ± 24.4
	15	-497.8 ± 110.2	987.8 ± 57.9	932.9 ± 71.2	645.6 ± 47.1	7.4 ± 8.7	8.7 ± 12.6
	16	-300.7 ± 206.59	1111.2 ± 19.5	1039.3 ± 34.6	734.8 ± 35.0	0.5 ± 1.9	0.9 ± 1.7
	16 w/ 26 kHz LPF	-794.8 ± 164.0	1162.1 ± 77.8	1063.2 ± 49.1	691.5 ± 25.74	-0.7 ± 0.2	1.2 ± 0.4

Table S4: Y-axis resolution study, per mille deviations for both the LeCroy and PicoScope DAQs at varied bit resolutions under pulsed buffer gas introduction mode.